The Journal of Immunology

IVIg Promote Cross-Tolerance against Inflammatory Stimuli In Vitro and In Vivo

Ángeles Domínguez-Soto, Miriam Simón-Fuentes, Mateo de las Casas-Engel, Víctor D. Cuevas, María López-Bravo, Jorge Domínguez-Andrés, Paula Saz-Leal, David Sancho, Carlos Ardavín, Juliana Ochoa-Grullón, Silvia Sánchez-Ramón, Miguel A. Vega and Angel L. Corbí

J Immunol 2018; 201:41-52; Prepublished online 9 May 2018;
doi: 10.4049/jimmunol.1701093
http://www.jimmunol.org/content/201/1/41

The Journal of Immunology is published twice each month by
The American Association of Immunologists, Inc.,
1451 Rockville Pike, Suite 650, Rockville, MD 20852

Print ISSN: 0022-1767 Online ISSN: 1550-6606.

IVIg Promote Cross-Tolerance against Inflammatory Stimuli In Vitro and In Vivo

Ángeles Domínguez-Soto,* Miriam Simón-Fuentes,* Mateo de las Casas-Engel,* Víctor D. Cuevas,* María López-Bravo,† Jorge Domínguez-Andrés,† Paula Saz-Leal,‡ David Sancho,‡ Carlos Ardavín,† Juliana Ochoa-Grullón,§ Silvia Sánchez-Ramón,§ Miguel A. Vega,* and Angel L. Corbí*

IVIg is an approved therapy for immunodeficiency and for several autoimmune and inflammatory diseases. However, the molecular basis for the IVIg anti-inflammatory activity remains to be fully explained and cannot be extrapolated from studies on animal models of disease. We now report that IVIg impairs the generation of human monocyte–derived anti-inflammatory macrophages by inducing JNK activation and activin A production and limits proinflammatory macrophage differentiation by inhibiting GM-CSF–driven STAT5 activation. In vivo, IVIg provokes a rapid increase in peripheral blood activin A, CCL2, and IL-6 levels, an effect that can be recapitulated in vitro on human monocytes. On differentiating monocytes, IVIg promotes the acquisition of altered transcriptional and cytokine profiles, reduces TLR expression and signaling, and upregulates negative regulators of TLR-initiated intracellular signaling. In line with these effects, in vivo IVIg infusion induces a state tolerant toward subsequent stimuli that results in reduced inflammatory cytokine production after LPS challenge in human peripheral blood and significant protection from LPS-induced death in mice. Therefore, IVIg conditions human macrophages toward the acquisition of a state of cross-tolerance against inflammatory stimuli, an effect that correlates with the net anti-inflammatory action of IVIg in vivo. ***The Journal of Immunology*****, 2018, 201: 41–52.**

Extensive macrophage accumulation is one of the hallmarks of inflammatory responses. During inflammation, monocytes egress from the bone marrow into the circulation (1, 2) and migrate into inflamed tissues (1, 3–5), where they give rise to distinct macrophage and dendritic cell subsets under the influence of tissue cellular and extracellular cues (6, 7). The high sensitivity of monocytes to the surrounding milieu is exemplified by their distinct responses to GM-CSF and M-CSF, which drive differentiation into functionally different macrophages (8). GM-CSF promotes proinflammatory macrophages (human monocyte–derived macrophages differentiated in the presence of GM-CSF [GM-MØ]) (9, 10) characterized by the expression of a "proinflammatory gene set" (11, 12). Conversely, M-CSF leads to tissue repair and anti-inflammatory/homeostatic macrophages (human monocyte–derived macrophages differentiated in the presence of M-CSF [M-MØ]) with robust IL-10–producing ability in response to pathogenic stimuli (9, 10, 13), which are transcriptionally defined by the expression of an "anti-inflammatory gene set" (11, 12, 14). Human GM-MØ and M-MØ are considered as proinflammatory and anti-inflammatory macrophages based on their respective profiles of stimuli-induced cytokines (9, 10, 15, 16) and because their specific gene signatures resemble those of macrophages from rheumatoid arthritis joints and tumor-associated macrophages, respectively (17). An adequate shift between the pro- and anti-inflammatory functions of macrophages is required for elimination of inflammatory insults and tissue repair (18, 19). Because deregulated macrophage polarization leads to the onset and maintenance of chronic inflammation (20–25), strategies for modulating macrophage polarization are of therapeutic use in chronic inflammatory diseases (26–30).

IVIg is a preparation of highly purified polyclonal and polyspecific IgG isolated from plasma of thousands of healthy donors. Besides substitutive treatment of patients with primary and secondary Ab deficiencies, IVIg is currently used in a large and growing number of autoimmune and systemic inflammatory disorders (31–34), as it exerts immunomodulatory effects on a variety of immune cells (31, 35, 36). Several non–mutually exclusive mechanisms have been proposed to explain the IVIg immunoregulatory action, including the sialic acid content of the Fc portion of the Abs and the interaction with ITAM-bearing Fc receptors (31, 32, 35–43). We have previously reported that IVIg

*Departamento de Biología Celular, Centro de Investigaciones Biológicas, Consejo Superior de Investigaciones Cientificas, 28040 Madrid, Spain; †Departamento de Inmunología y Oncología, Centro Nacional de Biotecnología, Consejo Superior de Investigaciones Cientificas, 28049 Madrid, Spain; ‡Fundación Centro Nacional de Investigaciones Cardiovasculares, Centro Nacional de Investigaciones Cardiovasculares, 28029 Madrid, Spain; and §Departamento de Inmunología Clínica, Hospital Universitario Clínico San Carlos, 28040 Madrid, Spain

ORCIDs: 0000-0002-2816-8070 (V.D.C.); 0000-0002-9091-1961 (J.D.-A.); 0000-0001-9585-6167 (S.S.-R.); 0000-0001-6151-4193 (M.A.V.).

Received for publication July 28, 2017. Accepted for publication April 18, 2018.

This work was supported by grants from the Ministerio de Economía y Competitividad (SAF2014-23801), the Instituto de Salud Carlos III (La Red de Investigación en Inflamación y Enfermedades Reumáticas, RIER RD12/009), and the Comunidad Autónoma de Madrid/FEDER (S2010/BMD-2350, RAPHYME Program) to A.L.C. and M.A.V. and by Instituto de Salud Carlos III Grant PI16/01428 to S.S.-R.

Address correspondence and reprint requests to Dr. Ángeles Domínguez-Soto and Dr. Angel L. Corbí, Centro de Investigaciones Biológicas, Consejo Superior de Investigaciones Cientificas, Ramiro de Maeztu, 9, 28040 Madrid, Spain. E-mail addresses: ads@cib.csic.es (Á.D.-S.) and acorbi@cib.csic.es (A.L.C.)

The online version of this article contains supplemental material.

Abbreviations used in this article: GM-BMDM, murine bone marrow–derived macrophage differentiated in the presence of GM-CSF; GM-MØ, human monocyte–derived macrophage differentiated in the presence of GM-CSF, proinflammatory macrophage; IVIg/GM-MØ, human monocyte–derived macrophage differentiated in the presence of GM-CSF and IVIg; IVIg/M-MØ, human monocyte–derived macrophage differentiated in the presence of M-CSF and IVIg; M-MØ, human monocyte–derived macrophage differentiated in the presence of M-CSF, anti-inflammatory/homeostatic macrophage; qRT-PCR, quantitative real-time PCR.

skews human and mouse macrophage polarization through FcγR-dependent mechanisms (44) and that the IVIg immunomodulatory activity is dependent on the polarization state of the responding macrophage, as IVIg limits the proinflammatory transcriptome and functions of GM-MØ but favors the acquisition of proinflammatory properties in M-MØ (44). In fact, IVIg potentiates inflammatory tissue-damaging responses in murine models of stroke and sepsis (44) and reduces tumor growth and metastasis in tumor models (44). However, extrapolation of the IVIg effects from animal models of disease to human pathology is not obvious because IVIg is prophylactically administered in most animal studies, whereas IVIg is used as a therapeutic strategy in humans (40).

We now report that IVIg modulates M-CSF– and GM-CSF–driven in vitro macrophage differentiation through distinct molecular mechanisms and conditions monocytes in vivo to acquire a state of tolerance against inflammatory stimuli. These findings provide novel insights into the anti-inflammatory activity of IVIg in vivo.

Materials and Methods

Macrophage differentiation, cell culture, and treatments

Human monocytes were purified from PBMCs by magnetic cell sorting using anti-CD14 microbeads (Miltenyi Biotec) (>95% $CD14^+$ cells) and cultured at 0.5×10^6 cells/ml for 7 d in RPMI 1640 supplemented with 10% FCS and either 1000 U/ml GM-CSF or 10 ng/ml M-CSF (ImmunoTools) to generate GM-MØ or M-MØ, respectively. Cytokines and IVIg (10 mg/ml; Privigen, CSL Behring) were added every 2 d, reaching 20–23 mg/ml of Igs at the end of the 7-d differentiation process. For activation, macrophages were treated with *Escherichia coli* 055:B5 LPS (10 ng/ml) for 24 h. Whenever indicated, a neutralizing Ab against human activin A (100 ng/ml; R&D Systems) was used. Murine bone marrow–derived macrophages differentiated in the presence of GM-CSF (GM-BMDMs) were generated using murine GM-CSF (1000 U/ml; PeproTech).

Quantitative real-time PCR

Total RNA was extracted using the RNeasy Mini Kit or the AllPrep DNA/RNA/Protein Mini Kit (Qiagen). cDNA was synthesized using the Reverse Transcription System kit (Applied Biosystems) (45). Oligonucleotides were designed with Universal ProbeLibrary software (Roche Life Sciences). Quantitative real-time PCR (qRT-PCR) was performed using custom-made microfluidic gene cards (Roche Life Sciences) or standard plates on a LightCycler 480 (Roche Life Sciences) (12). Where indicated, a panel of 28 genes differentially expressed between GM-MØ and M-MØ (and included within the previously defined proinflammatory gene set and anti-inflammatory gene set) was analyzed (11, 12). Assays were made in triplicate, and results were normalized according to the mean of the expression levels of *HPRT*, *SDHA*, and *TBP*. Results were expressed using the ΔΔCT method for quantitation.

Western blot

Cell lysates were subjected to SDS-PAGE and transferred onto an Immobilon-P polyvinylidene difluoride membrane (Millipore). After blocking the unoccupied sites with 5% BSA, protein detection was carried out with Abs against total and phosphorylated ERK1/2, total and phosphorylated JNK, IκBα, phosphorylated IRF3, phosphorylated STAT5, phosphorylated SHIP-1, A20 (Cell Signaling Technology), total and phosphorylated STAT1, phosphorylated STAT3 (BD Biosciences), or phosphorylated SHP-1 (Cell Signaling Technology) and using the SuperSignal West Pico Chemiluminescent system (Pierce). Protein loading was normalized using a mAb against GAPDH (sc-32233; Santa Cruz Biotechnology) or an Ab against human vinculin (Sigma-Aldrich).

Clinical samples and ex vivo LPS tolerance

Peripheral blood was obtained from 36 patients receiving IVIg therapy (400 mg/kg body weight), both before and after (5 h) IVIg infusion, and serum or plasma was recovered using standard procedures. Patients had been previously diagnosed with either common variable immunodeficiency and other inflammatory disorders ($n = 18$) or recurrent reproductive failure of inflammatory cause ($n = 18$). To assess cross-tolerance to LPS in ex vivo experiments, peripheral blood obtained from 10 patients receiving IVIg therapy, both before and after IVIg infusion, was maintained for 12 h at room temperature and treated with PBS or LPS (10 ng/ml) for 10 h, and plasma was recovered using standard procedures. Where indicated, monocytes were isolated from the peripheral blood of IVIg-treated patients using anti-CD14 microbeads (Miltenyi Biotec). All patients gave informed consent, and the Hospital Universitario Clínico San Carlos ethics committee approved the study.

In vivo endotoxin tolerance

For survival studies, mice ($n = 20$ mice per group) received PBS or IVIg i.p. (400 μl of a 100 mg/ml solution, 40 mg/mouse). After 26 h, mice were challenged i.p. with LPS (9 mg/kg in saline). Mouse survival was monitored every 12 h for 5 d. For survival studies, statistical analysis was performed using the Mantel–Cox log-rank test ($^{**}p < 0.01$).

Flow cytometry

Phenotypic analysis was carried out by flow cytometry as described previously (46) using either a mAb specific for human TLR4 (sc-13593; Santa Cruz Biotechnology) or an isotype-matched control Ab (Chemicon) and followed by staining with FITC-labeled Fab goat anti-mouse IgG. All incubations were done in the presence of 50 μg/ml human IgG to prevent binding through the Fc portion of the Abs.

ELISA

Culture supernatants from untreated or LPS-treated (24 h) human macrophages and plasma from patients were assayed for the presence of cytokines using a commercially available ELISA for human TNF-α, IL-12p40 (BD Pharmingen), CXCL10, IL-6, IL-10 (BioLegend), and activin A (R&D Systems). ELISA was performed following the protocols supplied by the manufacturers.

Statistical analysis

Unless otherwise indicated and for comparisons of means, statistical analysis was performed using the Student t test, and a p value <0.05 was considered significant ($^{*}p < 0.05$, $^{**}p < 0.01$, $^{***}p < 0.001$).

Results

IVIg blocks the acquisition of the anti-inflammatory transcriptional signature of M-MØ through JNK activation and activin A production

Peripheral blood monocytes are the immediate precursors of macrophages within inflamed tissues (47). Because IVIg modulates polarization of human macrophages (44), we sought to assess the IVIg effects on the ability of monocytes to differentiate into macrophages in vitro. To that end, monocytes were differentiated in the presence of therapeutic doses of IVIg. IVIg infusion as a replacement therapy (48) or as immunosuppressive therapy (31, 32, 36) raises peripheral blood IgG to 15–35 mg/ml (48–50) and increases IgG blood concentration by an average of 1.8-fold (mean of maximal IgG levels after IVIg infusion of 16.9 mg/ml). Therefore, monocytes were differentiated with either M-CSF or GM-CSF and with IVIg reaching a final concentration of 20–30 mg/ml at the end of the macrophage differentiation protocol. The presence of IVIg along M-CSF–driven differentiation generated macrophages (human monocyte–derived macrophages differentiated in the presence of M-CSF and IVIg [IVIg/M-MØ]) with significantly lower expression of the whole M-MØ–specific anti-inflammatory gene set and higher expression of several transcripts of the GM-MØ–specific proinflammatory gene set (Fig. 1A) (12, 51). The IVIg-induced transcriptomic changes were observed with IVIg concentrations as low as 1 mg/ml (Supplemental Fig. 1A) and were already detected 48 h after exposure to IVIg (Fig. 1B). The IVIg-induced changes were also evident at the protein level after 48 h of IVIg exposure, as indicated by the loss of expression of MAFB (Fig. 1C), which controls expression of most genes of the anti-inflammatory gene set (14), and the huge increase in the production of activin A (Fig. 1D), which drives the generation of

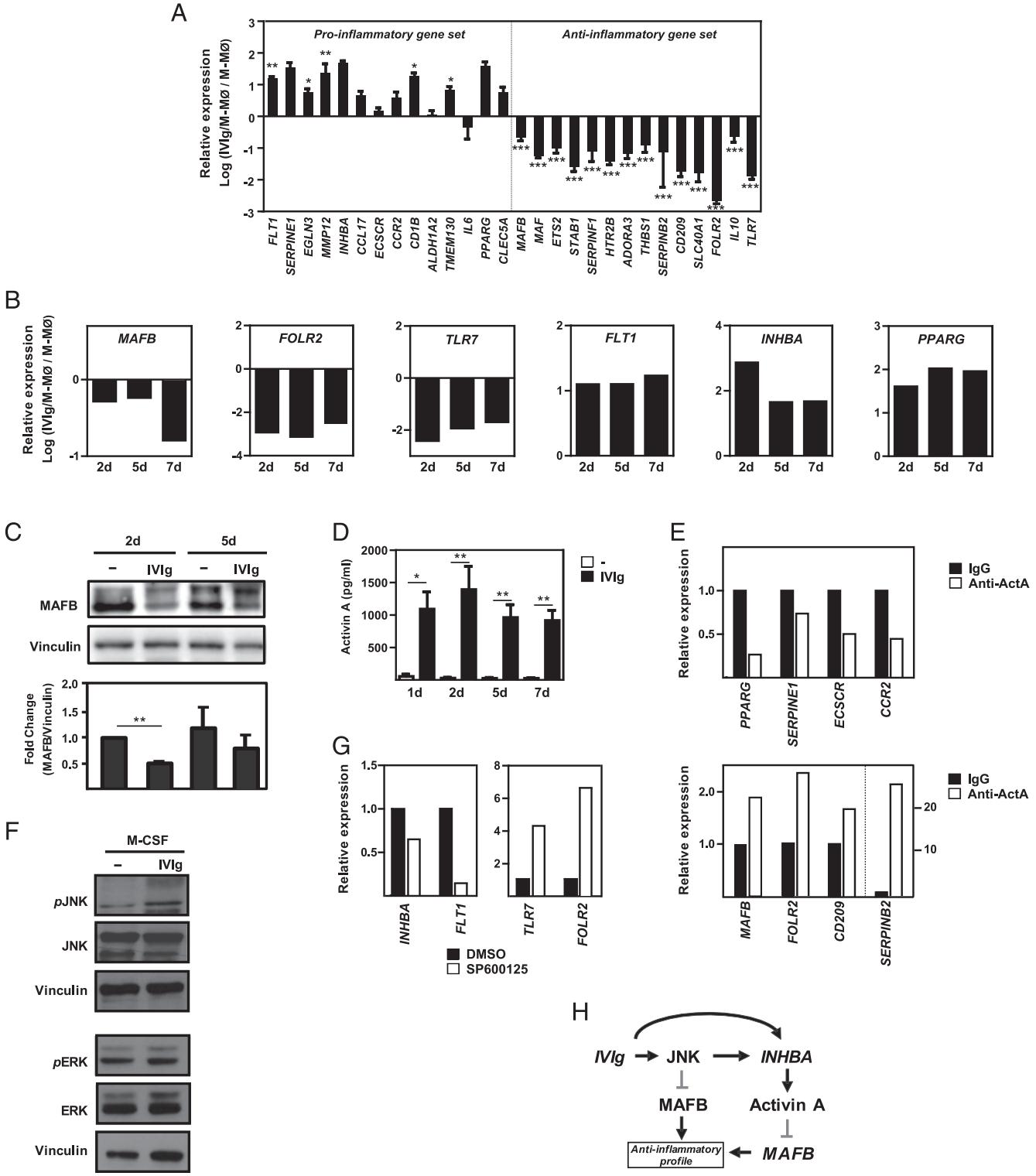

FIGURE 1. IVIg blocks the acquisition of the anti-inflammatory transcriptional signature of M-MØ through JNK activation and activin A production. (**A**) Relative expression of the indicated genes in IVIg/M-MØ, as determined by qRT-PCR. The experiment was done on monocytes from five independent donors, and shown is the mean ± SEM. (**B**) Expression of the indicated genes in monocytes differentiated under the influence of M-CSF with or without IVIg for 2, 5, or 7 d, as determined by qRT-PCR. Two independent experiments were performed and one of them is shown. In (A) and (B), results show the expression of each gene in IVIg/M-MØ relative to its expression in M-MØ. (**C**) Immunoblot analysis of MAFB protein levels in monocytes exposed to IVIg for 2 or 5 d. Protein levels of vinculin were determined in parallel to control for protein loading. Densitometric quantification of the relative MAFB protein levels in three independent experiments is shown in the lower panel. The expression of MAF in monocytes cultured for 2 d in the absence of IVIg was arbitrarily set to 1. (**D**) Activin A levels in culture supernatants of monocytes differentiated with M-CSF for the indicated periods of time and either in the absence or presence of IVIg. Each determination was performed in triplicate, and shown is the mean ± SEM of seven independent experiments. (**E**) Relative expression of the indicated genes in IVIg/M-MØ generated in the presence of 100 ng/ml of a blocking anti–activin A Ab (Anti-ActA) or an isotype-matched Ab (IgG), as determined by qRT-PCR. Shown are the relative mRNA levels of each gene (relative to *TBP* RNA levels) referred to its expression level when differentiation was done in the presence of an isotype-matched Ab (IgG). The experiment was done on monocytes from two independent donors, and one of the experiments is shown. (**F**) Immunoblot analysis of p-JNK, p-ERK, total JNK, and total ERK *(Figure legend continues)*

macrophages with proinflammatory activity (11, 12). The relevance of the IVIg-induced activin A production was demonstrated by the ability of a neutralizing anti–activin A Ab to partially reverse the IVIg-induced transcriptional changes (Fig. 1E). Moreover, IVIg/M-MØ–conditioned medium also exhibited an enhanced ability to limit tumor cell proliferation (data not shown), an activin A–dependent function that is exclusive to proinflammatory GM-MØ (12).

Regarding intracellular signaling, in M-CSF–exposed monocytes, IVIg did not affect the activation state of ERK or NF-κB (Fig. 1F, data not shown) but induced JNK phosphorylation (Fig. 1F), partly via Syk activation (Supplemental Fig. 2). The IVIg-induced JNK phosphorylation is particularly relevant because JNK activity drives the generation of macrophages with proinflammatory activity (52). In fact, the IVIg-induced transcriptional changes could also be impaired by inhibition of JNK activation, as evidenced by the weaker increase of *INHBA* (the activin A–encoding gene) and *FLT1* and the lower downregulation of *FOLR2* and *TLR7* (Fig. 1G). Because JNK activation contributes to *INHBA* expression (Fig. 1G) but also accelerates MAFB degradation (53), these results indicate that IVIg limits the transcriptional differentiation of monocytes into anti-inflammatory macrophages by triggering JNK activation and activin A production (Fig. 1H).

IVIg inhibits GM-CSF–induced STAT5 activation and impairs the acquisition of the GM-CSF–dependent transcriptional profile of proinflammatory GM-MØ

GM-CSF is a key driver of tissue inflammation whose levels are increased in blood from patients with inflammatory disorders, and it has become a therapeutic target in inflammatory diseases (54). We next evaluated the effect of IVIg on the GM-CSF–driven differentiation of human GM-MØ. The continuous presence of IVIg significantly impaired the upregulation of members of the proinflammatory gene set that characterizes proinflammatory GM-MØ (11, 12) (Fig. 2A) in a dose-dependent manner (Supplemental Fig. 1A). Like in the case of M-MØ, IVIg modulated gene expression after a single dose (48 h) (Fig. 2B). Interestingly, comparison of the transcriptional profile of macrophages generated in the absence or presence of IVIg revealed that the huge transcriptomic differences between GM-MØ and M-MØ (11, 12) are blunted when differentiation takes place in the continuous presence of IVIg and that IVIg/M-MØ exhibit a transcriptional profile that resembles the profiles of GM-MØ and human monocyte–derived macrophages differentiated in the presence of GM-CSF and IVIg (IVIg/GM-MØ) (Supplemental Fig. 1B). Thus, therapeutic concentrations of IVIg inhibit the transcriptional response of monocytes toward M-CSF or GM-CSF, impairing the generation of M-MØ or GM-MØ. In the case of GM-CSF–driven macrophage differentiation, IVIg exposure further increased the GM-CSF–induced phosphorylation of JNK in human monocytes (Fig. 2C, left panel). This IVIg-dependent enhancement of JNK activation did not translate into higher levels of activin A (Fig. 2A), probably because GM-CSF–induced JNK phosphorylation suffices to yield maximal INHBA gene expression. More importantly, IVIg drastically reduced the GM-CSF–induced STAT5 phosphorylation in human monocytes (Fig. 2C, right panel). Therefore, the ability of IVIg to impair the acquisition of the GM-CSF–dependent transcriptional profile correlates with its capacity to block STAT5 activation, which allows us to conclude that IVIg inhibits the transcriptional response of monocytes toward M-CSF or GM-CSF by distinct mechanisms.

IVIg disrupts the LPS responsiveness of proinflammatory GM-MØ and anti-inflammatory M-MØ

The defining functional feature of M-MØ and GM-MØ is their capacity to preferentially produce high levels of IL-10 and CCL2 (M-MØ) or proinflammatory cytokines (TNF-α, IL-12p40) (GM-MØ) in response to TLR ligands (13). Thus, we next compared the LPS responsiveness of macrophages generated in the absence (M-MØ, GM-MØ) or presence of IVIg (IVIg/M-MØ, IVIg/GM-MØ). Compared to M-MØ, IVIg/M-MØ exhibited a significantly lower production of LPS-induced CCL2, IL-10, and CXCL10 (reduction of LPS inducibility to 4.5% in M-MØ, $p = 3 \times 10^{-4}$) (Fig. 3A, left panels) as well as higher levels of LPS-induced TNF-α and IL-12p40 (Supplemental Fig. 1C). The distinct cytokine response of M-MØ and IVIg/M-MØ was also evident upon exposure to TLR2 ligands such as Pam3Cys or lipoteichoic acid (Fig. 3A, left panels). By contrast, IVIg/GM-MØ displayed a significantly lower LPS-induced expression of TNF-α, IL-12p40, CXCL10 (reduction of LPS inducibility to 0.06% in GM-MØ, $p = 2 \times 10^{-7}$) (Fig. 3A, right panels), IL-10, and IL-6 (Supplemental Fig. 1C), and a similar reduction was also observed in response to TLR2 ligands (Fig. 3A, right panels). Moreover, the effect of IVIg was not limited to stimuli-induced cytokines because assessment of the expression of genes whose LPS inducibility is cell type–specific (V.D. Cuevas and A.L. Corbí, unpublished observations) revealed that LPS enhanced the expression of *NLRP3* in IVIg/M-MØ (a property that is unique to GM-MØ), whereas *LMNB1* expression (whose LPS inducibility is M-MØ-specific) was not upregulated by LPS in IVIg/M-MØ (Fig. 3B). Furthermore, LPS treatment reduced *LMNB1* expression in IVIg/GM-MØ (but not in GM-MØ) and upregulated *NLRP3* expression in GM-MØ (but not in IVIg/GM-MØ) (Fig. 3B). Therefore, therapeutic concentrations of IVIg severely modify the LPS responsiveness of macrophages generated in the presence of either M-CSF or GM-CSF.

Monocyte exposure to IVIg impairs LPS-initiated signaling and enhances the expression of negative regulators of NF-κB signaling

To identify the molecular basis for the IVIg ability to disrupt the LPS-induced cytokine production in human macrophages, we analyzed whether IVIg alters LPS-initiated intracellular signals. IVIg/M-MØ exhibited lower levels of LPS-induced ERK activation and IκBα degradation than M-MØ (Fig. 4A, left panels), and a similar result was found upon LPS stimulation of IVIg/GM-MØ and GM-MØ (Fig. 4A, right panels). The LPS-induced activation of IRF3 and STAT3 was also significantly lower in IVIg/M-MØ and IVIg/GM-MØ than in M-MØ and GM-MØ (Fig. 4B). Moreover, and in line with the diminished production of LPS-induced CXCL10 (Fig. 3A), the LPS-induced activation of STAT1 was

in monocytes cultured with M-CSF overnight, starved for 2 h in M-CSF–free and serum-free medium, and then treated with IVIg before stimulation with M-CSF for 15 min. Protein levels of ERK, JNK, and vinculin were determined in parallel to control for protein loading. In each case, three independent experiments were performed, and one experiment is shown. (**G**) Relative expression of the indicated genes in IVIg/M-MØ generated in the absence (DMSO) or in the presence of the JNK inhibitor SP600125 (30 μM), as determined by qRT-PCR. Shown are the relative mRNA levels of each gene (relative to *TBP* RNA levels) referred to its expression level when differentiation was done in the presence of DMSO. Three independent experiments were done and one of them is shown. (**H**) Schematic representation of the effects of IVIg on the acquisition of the anti-inflammatory gene profile by human monocytes. $*p < 0.05$, $**p < 0.01$, $***p < 0.001$.

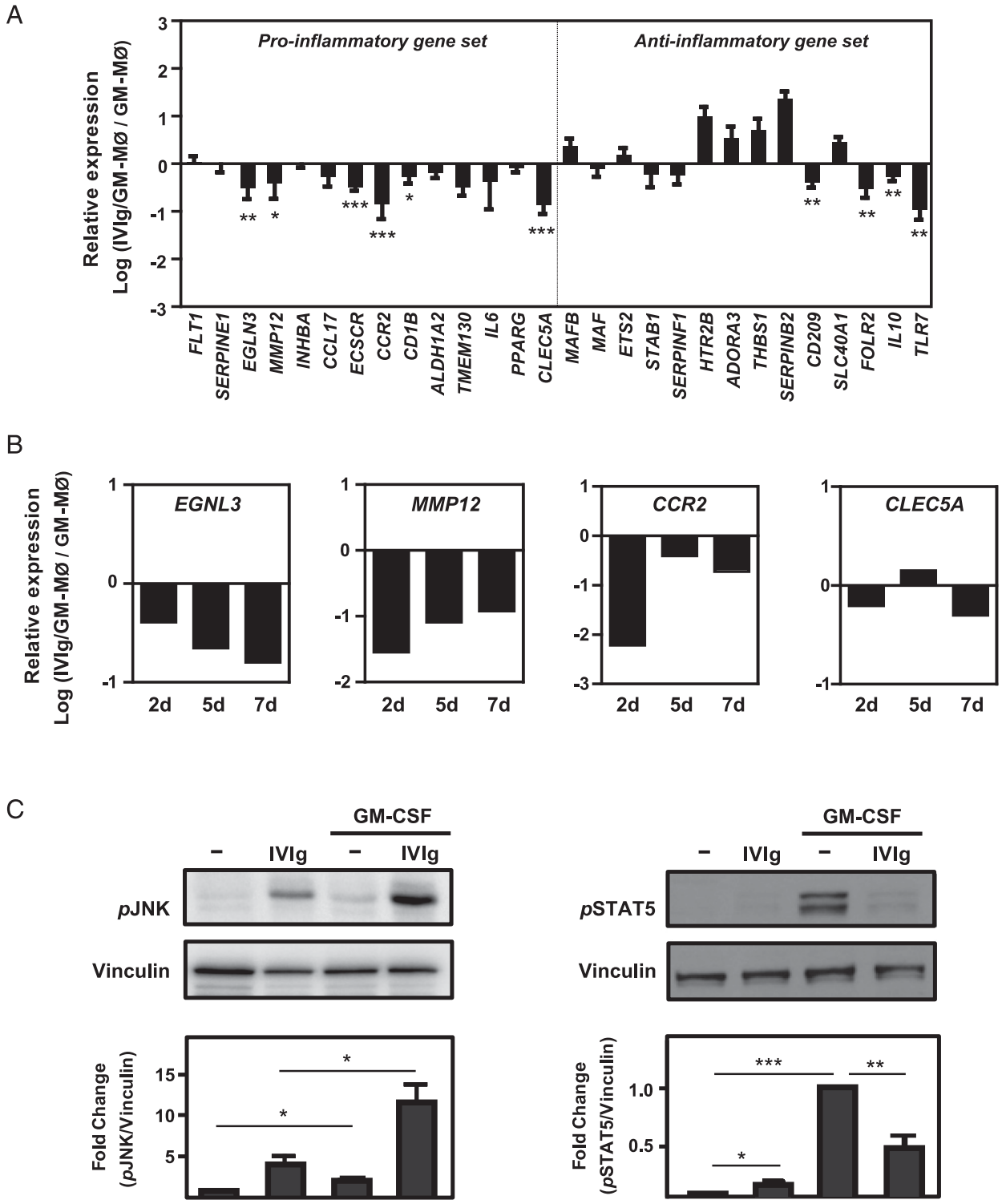

FIGURE 2. IVIg impairs the acquisition of the proinflammatory transcriptional signature of GM-MØ. (**A**) Relative expression of the indicated genes in IVIg/GM-MØ, as determined by qRT-PCR. The experiment was done on monocytes from five independent donors, and shown is the mean ± SEM. (**B**) Kinetics of the expression of the indicated genes along the differentiation of IVIg/GM-MØ, as determined by qRT-PCR. Two experiments were done on macrophages from independent donors, and one of them is shown. In (A) and (B), results show the expression of each gene in IVIg/GM-MØ relative to its expression in GM-MØ. (**C**) Immunoblot analysis of p-JNK (left panel) and p-STAT5 (right panel) in freshly isolated human monocytes untreated (-) or treated with IVIg before stimulation with GM-CSF for 15 min (for p-JNK) or 2 h (for p-STAT5). Protein levels of vinculin were determined in parallel to control for protein loading. Three independent experiments were performed whose densitometric analyses are shown. $*p < 0.05$, $**p < 0.01$, $***p < 0.001$.

also lower in IVIg/M-MØ and IVIg/GM-MØ (Fig. 4B). The weaker LPS-initiated signaling seen in macrophages generated in the presence of IVIg correlated with a diminished TLR4 cell surface expression (Fig. 4C) and reduced *TLR4* mRNA levels (Fig. 4D) in both IVIg/M-MØ and IVIg/GM-MØ. Therefore, the presence of therapeutic levels of IVIg during macrophage differentiation imposes a strong reduction in the signaling pathways that drive LPS-induced cytokine expression.

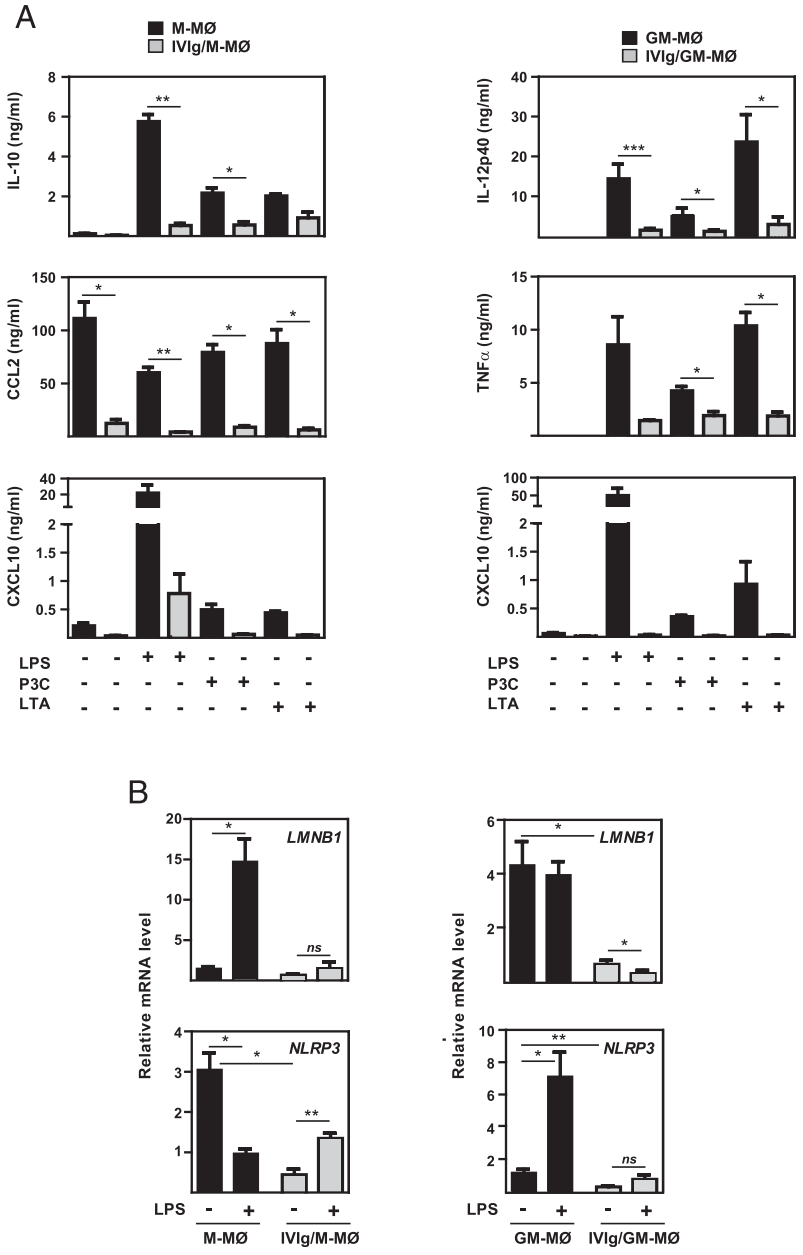

FIGURE 3. IVIg alters TLR responsiveness of M-MØ and GM-MØ. (**A**) Production of IL-10, CCL2, and CXCL10 in M-MØ and IVIg/M-MØ (left panels) or TNF-α, IL12p40, and CXCL10 in GM-MØ and IVIg/GM-MØ (right panels) that were either left untreated (-) or stimulated with 10 ng/ml LPS, 10 μg/ml Pam3CSK4, or 5 μg/ml LTA for 24 h, as determined by ELISA. Each determination was done in triplicate, and shown is the mean ± SEM of three independent experiments. (**B**) *NLRP3* and *LMNB1* mRNA expression levels in untreated (-) and LPS-treated (10 ng/ml, 4 h) M-MØ, IVIg/M-MØ, GM-MØ, and IVIg/GM-MØ, as determined by qRT-PCR. Results are expressed as relative mRNA levels (relative to *TBP* RNA levels). Mean ± SEM of three independent experiments is shown. $*p < 0.05$, $**p < 0.01$, $***p < 0.001$.

The fact that IVIg treatment leads to lower LPS-induced signaling and cytokine production is reminiscent of the endotoxin tolerance phenomenon (55). In fact, the acquisition of an LPS refractory state is compatible with the lower level of cell surface TLR4 and the weaker LPS-induced NF-κB activation seen in IVIg/M-MØ and IVIg/GM-MØ (Fig. 4A, 4C). To provide evidence for an IVIg-induced LPS refractory state in human macrophages, the expression and activation states of negative regulators of the LPS-initiated signaling pathway were assessed in IVIg/M-MØ and IVIg/GM-MØ. Compared with M-MØ, IVIg/M-MØ exhibited a higher expression of A20, an inhibitor of NF-κB activation (55) (Fig. 4E). Similarly, and compared with GM-MØ, IVIg/GM-MØ contained 1) higher levels of p-SHIP-1, which controls the PI3K cellular signaling pathway (56, 57); 2) considerably higher levels of A20, which inhibits NF-κB activation and contributes to limiting inflammation (58); and 3) higher levels of p-SHP-1, which negatively regulates TLR-mediated production of proinflammatory cytokines via inhibition of NF-κB and MAPK activation (59) (Fig. 4F). Therefore, macrophages generated in the presence of IVIg exhibit a number of features (diminished LPS-triggered intracellular signaling, reduced TLR4 expression, and higher p-SHIP-1, p-SHP-1, and A20 expression) that are compatible with IVIg promoting a state of cross-tolerance to LPS on differentiating monocytes.

IVIg treatment leads to a state of cross-tolerance to LPS in mice

Although IVIg exerts anti-inflammatory actions in mouse models of inflammatory disease (60, 61), its mechanisms of action differ between human and mouse, and results obtained with IVIg in mouse animal models of disease cannot be easily extrapolated (40). Despite this, we initially turned to the mouse system to determine the cell surface receptors implicated in the IVIg action and to assess the potential ability of IVIg to promote cross-tolerance to LPS. IVIg was found to modulate the phenotypic and functional profile of proinflammatory GM-BMDM (51, 62), as IVIg/GM-BMDM showed altered expression of polarization-specific genes (*Inhba, Clu, Emr1*) (51) (Fig. 5A) and produced

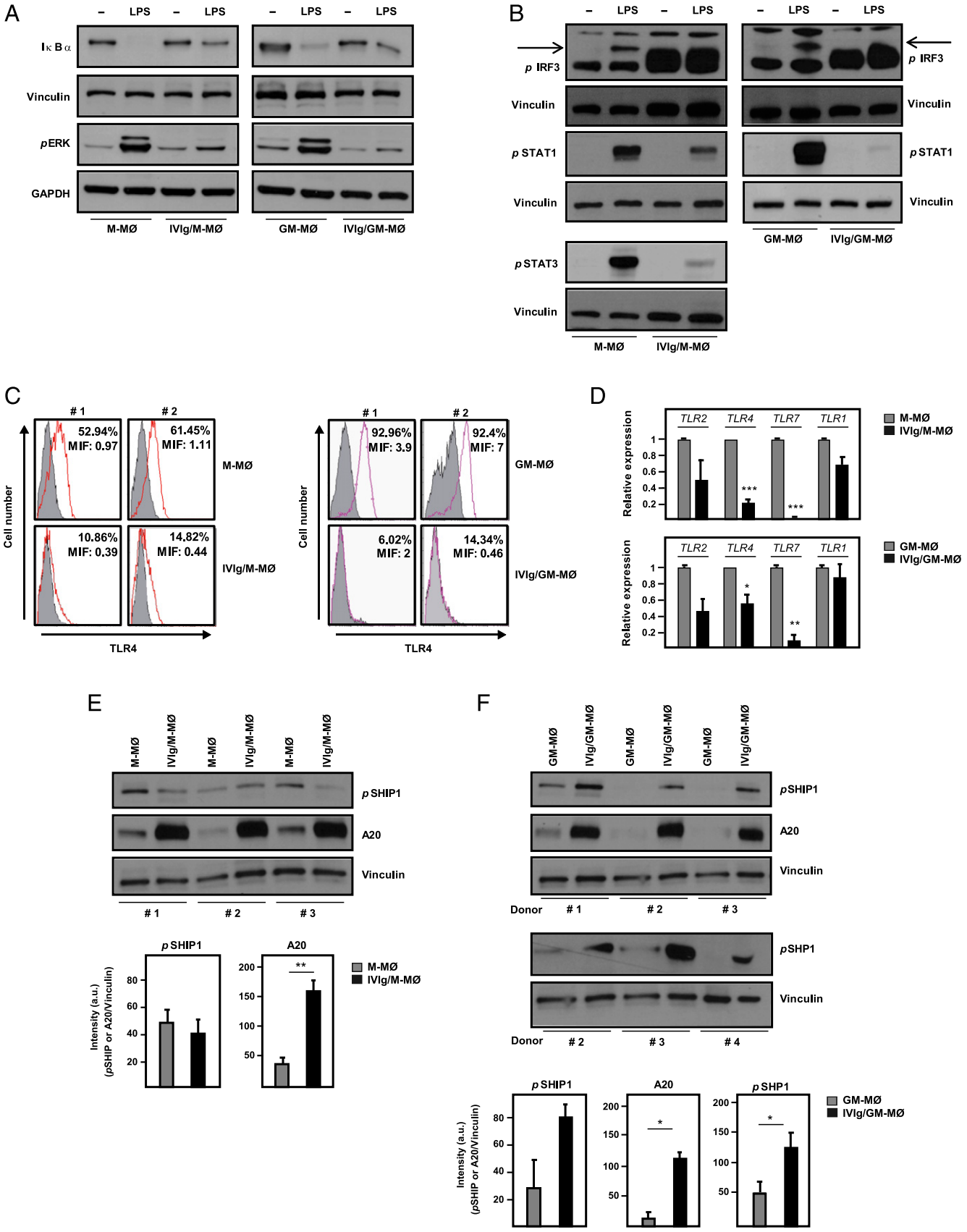

FIGURE 4. Human macrophage differentiation in the presence of IVIg impairs TLR4 signaling and enhances the expression of negative regulators of NF-κB signaling. (**A**) Immunoblot analysis of IκBα and p-ERK in M-MØ, IVIg/M-MØ (left panels), GM-MØ, and IVIg/GM-MØ (right panels) that were either untreated (-) or treated with 10 ng/ml LPS for 15 min. (**B**) Immunoblot analysis of p-IRF3, p-STAT3, and p-STAT1 in M-MØ, IVIg/M-MØ (left panels), GM-MØ, and IVIg/GM-MØ (right panels) that were either untreated (-) or treated with 10 ng/ml LPS for 2 h. Protein levels of GAPDH, STAT1, and vinculin were determined in parallel to control for protein loading. In each case, three independent experiments were performed, and one experiment is shown. (**C**) Cell surface expression of TLR4 (empty histograms) in M-MØ and IVIg/M-MØ (left panels) or GM-MØ and *(Figure legend continues)*

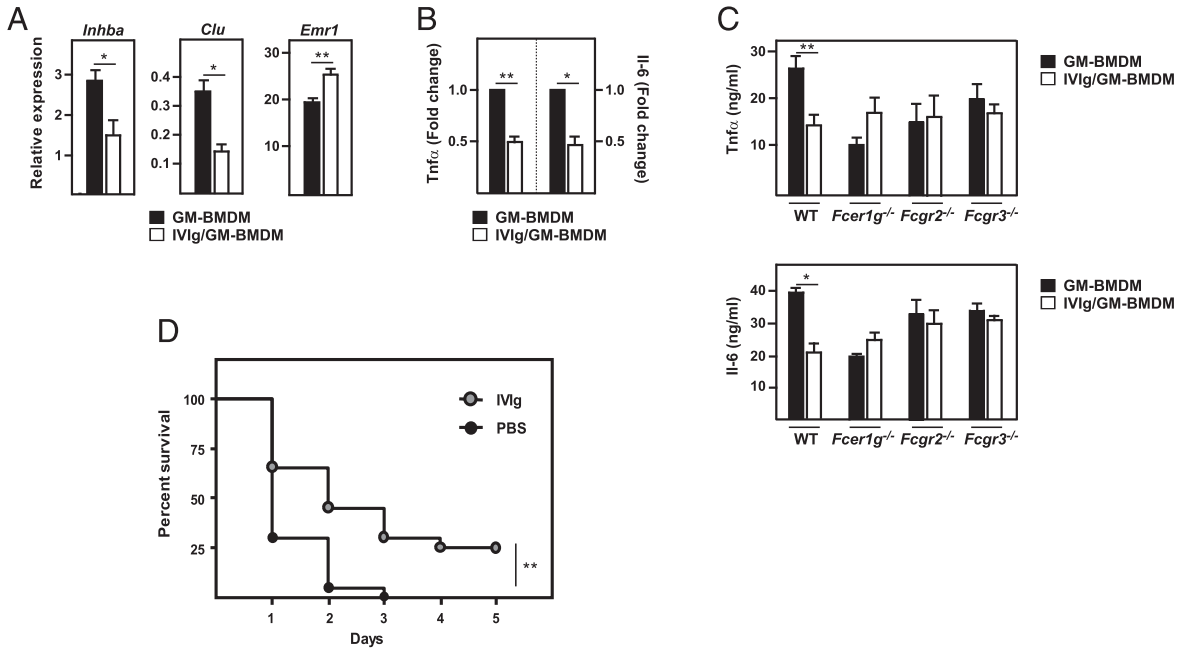

FIGURE 5. Effects of IVIg on mouse GM-BMDM differentiation and LPS responses in vivo. (**A**) Expression of polarization-associated genes in GM-BMDM and IVIg/GM-BMDM generated from C57BL/6 bone marrow, as determined by qRT-PCR. Relative expression indicates the expression of each marker relative to the expression of the *Tbp* gene. Shown is the mean ± SEM of three independent experiments. (**B**) LPS-induced release of Tnf-α and Il-6 from GM-BMDM and IVIg/GM-BMDM. Each determination was done in triplicate, and shown is the mean ± SEM of three independent experiments. (**C**) LPS-induced release of Tnf-α and Il-6 from GM-BMDM and IVIg/GM-BMDM generated from the bone marrow of wild type (WT), *Fcer1g*$^{-/-}$, *Fcgr2*$^{-/-}$, and *Fcgr3*$^{-/-}$ mice. Each determination was done in triplicate, and shown is the mean ± SEM of four independent experiments. (**D**) Survival of C57BL/6 mice pretreated with PBS or IVIg (40 μg/mouse) and then challenged 26 h later with a lethal dose of LPS (9 mg/kg). *$p < 0.05$, **$p < 0.01$.

lower levels of LPS-induced Tnf-α and Il-6 (Fig. 5B). The latter effects were dependent on Fcγ receptors, as deletion of *Fcgr3*, *Fcgr2*, or *Fcer1g* prevented the IVIg-mediated decrease in the LPS-induced secretion of Tnf-α and Il-6 (Fig. 5C), thus demonstrating that functional activating Fcγ receptors are required for the IVIg inhibition on the acquisition of proinflammatory functions in mouse macrophages. Because IVIg exerts a similar functional effect on human and mouse macrophages in vitro, the ability of IVIg to promote cross-tolerance to LPS was assessed using the endotoxin shock mouse model. To that end, mice were i.p. treated with IVIg (400 μl, 100 mg/ml) 26 h before receiving an i.p. injection of a lethal dose of LPS. IVIg-treated mice exhibited significantly higher survival than mice that had been pretreated with PBS (Fig. 5D). Therefore, in agreement with its ability to limit macrophage responses to LPS in vitro, IVIg is capable of inducing a state of endotoxin tolerance in mice.

IVIg infusion enhances inflammatory cytokine levels in peripheral blood

To evaluate whether IVIg can also promote tolerance to LPS in vivo in patients receiving IVIg therapy, we initially determined the ability of IVIg to alter the production of inflammatory cytokines in vivo. Cytokine determination on the peripheral blood of IVIg-treated patients with either immunodeficiency/inflammatory pathologic conditions (in which IVIg infusion increases IgG concentration from 11 to 19 mg/ml) (Fig. 6A, left panel) or recurrent reproductive failure of inflammatory causes (in which IVIg increases IgG concentration from 9.4 to 14.6 mg/ml) revealed a significant increase of IL-6, CCL2, and activin A 5 h after IVIg infusion (Fig. 6A, right panel). In vitro assessment of monocyte responses to IVIg (10 mg/ml) showed that IVIg is also capable of increasing the production of activin A, CCL2, and IL-6 from CD14$^+$ monocytes from healthy donors (Fig. 6B). Therefore, infusion of IVIg results in enhanced levels of activin A, CCL2, and IL-6 in peripheral blood. Because the production of these cytokines by monocytes also increased after IVIg treatment in vitro, these results are compatible with IVIg promoting tolerance toward other stimuli in vivo.

IVIg infusion promotes monocytes to acquire tolerance toward inflammatory stimuli

The ability of IVIg to induce tolerance in vivo was then evaluated through the analysis of blood samples obtained from IVIg-treated patients. In the first set of experiments, CD14$^+$ and CD14$^-$ cells

IVIg/GM-MØ (right panels) from two independent donors, as determined by flow cytometry. Background fluorescence was determined using an isotype-matched Ab (gray histograms). The percentages of marker-positive cells and mean intensity of fluorescence (MIF) are indicated in each case. (**D**) Relative expression of the indicated TLR genes in M-MØ and IVIg/M-MØ (upper panel) and GM-MØ and GM-MØ plus IVIg (lower panel), as determined by qRT-PCR. Results are expressed as relative expression (relative to *TBP* mRNA levels) and refer to the expression level of each gene in GM-MØ. Shown is the mean ± SEM of three independent experiments. (**E**) Immunoblot analysis of p-SHIP-1 and A20 on M-MØ and IVIg/M-MØ derived from three independent monocyte preparations. Protein levels of vinculin were determined in parallel to control for protein loading. Densitometric quantification of the immunoblots relative to vinculin levels is shown in the lower panel. (**F**) Immunoblot analysis of p-SHIP-1, A20, and p-SHP-1 on GM-MØ and IVIg/GM-MØ derived from three independent monocyte preparations. Protein levels of vinculin were determined in parallel to control for protein loading. Densitometric quantification of the immunoblots relative to vinculin levels is shown in the lower panel. *$p < 0.05$, **$p < 0.01$, ***$p < 0.001$.

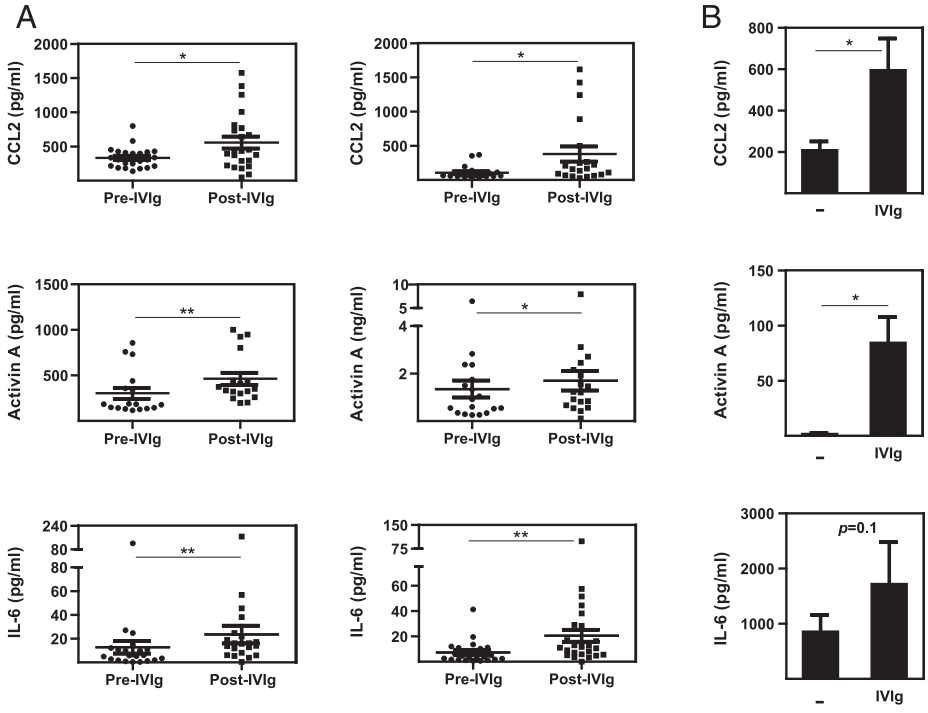

FIGURE 6. IVIg infusion leads to increased levels of inflammatory cytokines in peripheral blood in vivo and in monocytes in vitro. (**A**) Activin A, CCL2, and IL-6 levels in plasma or serum of patients with common variable immunodeficiency and other inflammatory disorders (n = 18, left panels) or recurrent reproductive failure of inflammatory cause (n = 18, right panels), both before (pre-IVIg) and 5 h after IVIg infusion (post-IVIg). Each determination was performed in triplicate, and shown is the mean ± SEM. (**B**) Activin A, CCL2, and IL-6 levels produced by $CD14^+$ monocytes from healthy subjects and either untreated (-) or exposed to IVIg (10 mg/ml) for 5 h. Eight independent experiments were performed, and shown is the mean ± SEM. $*p < 0.05$, $**p < 0.01$.

were isolated from the peripheral blood of patients both before and after IVIg infusion, and the production of LPS-induced TNF-α and IL-6 was determined in vitro. As shown in Fig. 7A and 7B, both cytokines were exclusively produced by $CD14^+$ monocytes, and more importantly, the LPS-upregulated levels of both cytokines were significantly lower in $CD14^+$ monocytes isolated from post-IVIg blood samples. Therefore, IVIg infusion renders monocytes less responsive toward a later stimulation by LPS. Next, and to confirm the induction of IVIg-mediated tolerance to LPS in whole blood, samples of peripheral blood were collected from patients both before and after IVIg infusion, maintained at room temperature for 12 h, and later challenged with either PBS or

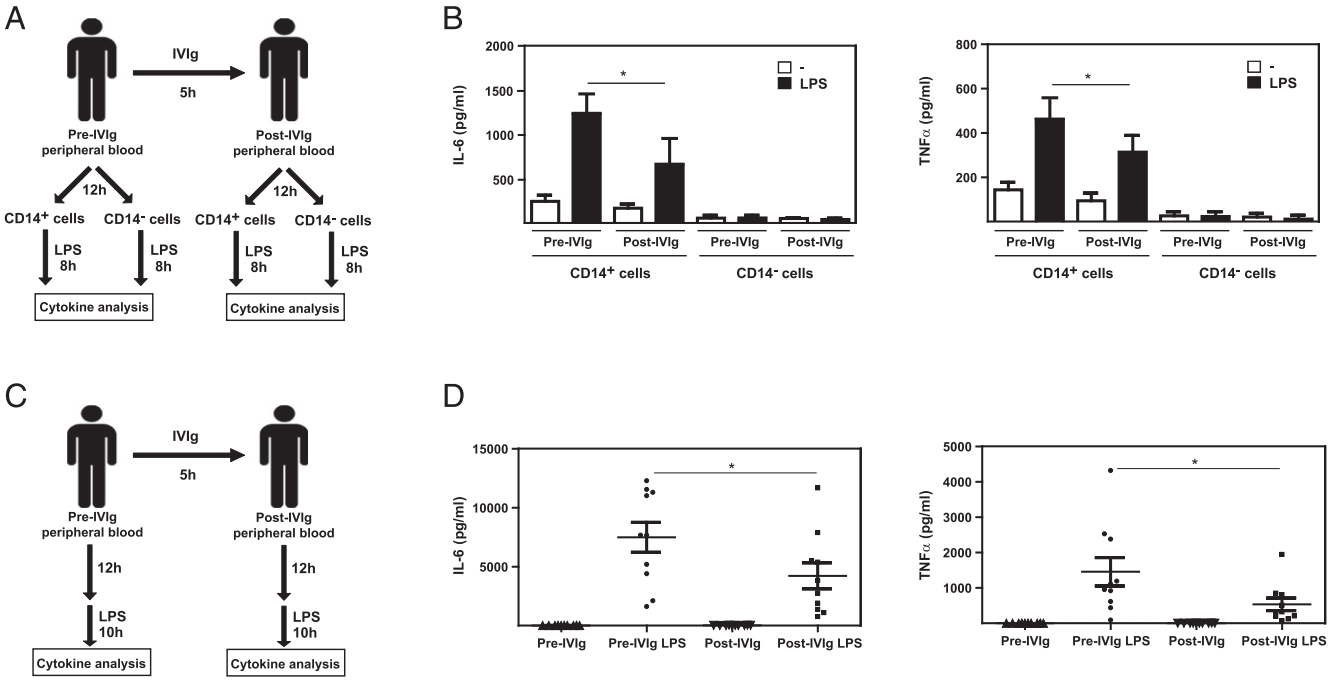

FIGURE 7. In vivo IVIg infusion promotes tolerance toward LPS. (**A**) Schematic representation of the experimental procedure used to assess LPS responsiveness of $CD14^+$ and $CD14^-$ cells isolated from the peripheral blood of IVIg-treated patients. (**B**) Whole blood was collected from IVIg-treated patients both before (pre-IVIg) and after receiving IVIg infusion (post-IVIg). After 12 h, $CD14^+$ and $CD14^-$ cells were isolated and treated with PBS (-) or LPS, and the levels of TNF-α and IL-6 were determined 8 h after stimulation. Each determination was performed in triplicate, and shown is the mean ± SEM of seven independent experiments. (**C**) Schematic representation of the experimental procedure used to assess IVIg-induced tolerance to LPS in the peripheral blood of IVIg-treated patients. (**D**) Whole blood was collected from IVIg-treated patients both before (pre-IVIg) and after receiving IVIg infusion (post-IVIg). After 12 h, blood was treated with PBS or LPS, and the levels of TNF-α and IL-6 were determined 10 h after stimulation. Each determination was performed in triplicate, and shown is the mean ± SEM of 10 independent experiments. $*p < 0.05$.

LPS (Fig. 7C). TNF-α and IL-6 were exclusively detected in LPS-treated blood samples, but significantly lower levels of both cytokines were found in the blood samples collected after IVIg infusion (Fig. 7D). Therefore, infusion of IVIg results in weaker proinflammatory cytokine response toward LPS in vivo, and this effect can be fully recapitulated with peripheral blood monocytes ex vivo (Fig. 7B). These results confirm that IVIg is capable of inducing a state of cross-tolerance to LPS in vivo and lead to the proposal that promotion of cross-tolerance toward other pathologic inflammatory stimuli underlies the net anti-inflammatory effect exerted by IVIg in vivo.

Discussion

The immunomodulatory action of IgG has widened the range of pathologic conditions for which IVIg therapy is either approved or has shown benefit (63, 64). Because of its beneficial actions on inflammatory pathologic conditions and its ability to limit tumor progression (44, 65, 66), we hypothesized that IVIg exerts its therapeutic action through modulation of the macrophage polarization state, whose deregulated control contributes to chronic inflammatory pathologic conditions, and found that IVIg shifts macrophage polarization at the functional and transcriptional levels (44). We now report that IVIg impairs the monocyte priming ability of M-CSF or GM-CSF through JNK activation and enhancement of activin A production (in the case of M-CSF) and also inhibits the GM-CSF–induced STAT5 activation. Besides, IVIg impairs the acquisition of the specific gene profiles and the TLR responses of proinflammatory and anti-inflammatory monocyte-derived macrophages. Importantly, the ability of IVIg to alter the LPS-induced macrophage cytokine profile correlates with the appearance of molecular parameters that limit TLR-initiated intracellular signaling and that characterize the state of endotoxin tolerance. In fact, we present evidence that IVIg promotes tolerance to LPS (cross-tolerance) in an endotoxin shock mouse model in vivo and that IVIg infusion results in weaker proinflammatory cytokine responses toward LPS in the peripheral blood of IVIg-treated patients.

Molecular analysis of the effects of IVIg has also led us to demonstrate that IVIg limits numerous intracellular signaling pathways in both human monocytes (GM-CSF–initiated STAT5 activation) and GM-MØ (LPS-triggered ERK, NF-κB, STAT1, and IRF3 activation). Blockade of intracellular signaling pathways is a common strategy for induction of tolerance. In the case of IVIg-treated human macrophages, the acquisition of the cross-tolerance state correlates with the appearance of molecular parameters that characterize desensitization in response to an inflammatory stimulus. Specifically, IVIg exposure results in lower TLR4 expression and higher levels of p-SHIP-1, p-SHP-1, and A20, all of which impair or inhibit LPS-triggered intracellular signaling. Therefore, IVIg shares with other tolerance-inducing agents the ability of increasing the expression of negative regulators of NF-κB signaling. Thus, A20 has been found to be partly responsible for the IVIg suppression of RANKL-induced osteoclastogenesis and TNF-α–induced bone resorption after engagement of Fcγ receptors (67). Therefore, similar to the case of LPS on human macrophages, IVIg might also induce a cross-tolerance state for RANKL and TNF-α, which share the NF-κB–activating activity with LPS.

The ability of IVIg to promote a tolerance state in macrophages can also explain its cell context–dependent effects. We previously showed that IVIg inhibits the proinflammatory functions of GM-MØ but enhances proinflammatory properties in M-MØ (44) and concluded that IVIg effects are cell type–dependent. However, NF-κB activation contributes to proinflammatory cytokine production in GM-MØ and IL-10 production in M-MØ. Considering that IVIg impairs NF-κB activation through the increase of negative regulators of NF-κB in both GM-MØ and M-MØ, this common molecular mechanism might underlie the opposite outcome of IVIg exposure in both types of macrophages: lower inflammatory cytokine production in GM-MØ and lower IL-10 production in M-MØ. Therefore, the opposite consequences of IVIg exposure to GM-MØ and M-MØ appear to be primarily a consequence of the distinct effector functions of both macrophage subtypes.

The capacity of IVIg to enhance the release of monocyte-derived cytokines, both in vitro and in vivo, clearly illustrates its monocyte-activating ability. The finding that activin A is one of the IVIg-induced cytokines has relevant implications and might also contribute to reconcile the pro- and anti-inflammatory actions of IVIg previously reported. Activin A is a member of the TGF-β family of factors (68) whose expression is high in inflammatory pathologic conditions (e.g., inflammatory bowel disease, rheumatoid arthritis, bacterial septicemia) and is induced with faster kinetics than other proinflammatory cytokines after LPS IV injection (69). Interestingly, activin A modulates inflammatory responses because it displays both proinflammatory and regulatory activities that resemble those exhibited by IVIg. Therefore, it is tempting to speculate that activin A critically contributes to the in vivo actions of IVIg. An additional implication of the IVIg-promoted increase of activin A relates to the function of activin A in promoting oocyte maturation, endometrial repair, decidualization, and maintaining pregnancy and to the fact that deregulation of the activin activities results in disorders of female reproduction and pregnancy (70). Previous reports indicate that low-dose IVIg overcome recurrent spontaneous abortions in women suffering from IgG subclass deficiency (71) and enhance clinical pregnancy and live birth rates in patients with recurrent reproductive failure of inflammatory cause (72). Therefore, the increase in activin A blood levels secondary to IVIg infusion might also contribute to the beneficial effects of IVIg on women with recurrent reproductive failure, a hypothesis that deserves further studies.

Numerous molecular and cellular mechanisms have been previously proposed to contribute to the IVIg immunoregulatory activity (31, 35, 37). The results reported in this article indicate that monocytes (and monocyte-derived macrophages) are involved in the effects of IVIg in vivo because IVIg infusion enhances the levels of monocyte-derived cytokines (e.g., activin A, CCL2, IL-6) in peripheral blood and alters the monocyte cytokine profile and macrophage differentiation capability in vitro. Therefore, IVIg targets monocytes (and monocyte-derived macrophages) and leads to the acquisition of a cross-tolerance state that underlies the apparent contradiction between its proinflammatory effects on monocytes and M-MØ in vitro and its immunosuppressive action in vivo (32, 41). According to this explanation, IVIg would shift monocytes/macrophages toward the acquisition of a proinflammatory profile, making IVIg-conditioned cells less sensitive to a subsequent exposure to TLR ligands. Consequently, IVIg-primed monocytes would be weakly responsive to further stimulation by any danger signals (e.g., TLR ligands) found after their entry into inflamed tissues. Therefore, monocyte exposure to IVIg would result in a lower level of macrophage activation within inflamed tissues and, consequently, would limit tissue damage (and pathologic conditions) triggered by an ongoing injury or an inflammation-provoking insult (danger signals or inflammatory stimuli). This hypothesis is supported by the ability of IVIg infusion to trigger an almost immediate increase in the level of inflammatory cytokines in peripheral blood, a result also reported by others (73, 74), and is compatible with the well-known therapeutic

benefits of IVIg in diseases like Kawasaki disease (75) and demyelinating polyneuropathy/Guillain–Barré syndrome (76), in which macrophages contribute to pathologic conditions.

Acknowledgments

We thank Dr. W.G. Kerr (State University of New York Upstate Medical University, Syracuse, NY) for providing SHIP-1 knockout mice.

Disclosures

The authors have no financial conflicts of interest.

References

1. Geissmann, F., M. G. Manz, S. Jung, M. H. Sieweke, M. Merad, and K. Ley. 2010. Development of monocytes, macrophages, and dendritic cells. *Science* 327: 656–661.
2. Fogg, D. K., C. Sibon, C. Miled, S. Jung, P. Aucouturier, D. R. Littman, A. Cumano, and F. Geissmann. 2006. A clonogenic bone marrow progenitor specific for macrophages and dendritic cells. *Science* 311: 83–87.
3. Chow, A., B. D. Brown, and M. Merad. 2011. Studying the mononuclear phagocyte system in the molecular age. *Nat. Rev. Immunol.* 11: 788–798.
4. Epelman, S., K. J. Lavine, and G. J. Randolph. 2014. Origin and functions of tissue macrophages. *Immunity* 41: 21–35.
5. Gomez Perdiguero, E., and F. Geissmann. 2013. Myb-independent macrophages: a family of cells that develops with their tissue of residence and is involved in its homeostasis. *Cold Spring Harb. Symp. Quant. Biol.* 78: 91–100.
6. Gordon, S., and P. R. Taylor. 2005. Monocyte and macrophage heterogeneity. *Nat. Rev. Immunol.* 5: 953–964.
7. Mosser, D. M., and J. P. Edwards. 2008. Exploring the full spectrum of macrophage activation. [Published erratum appears in 2010 *Nat. Rev. Immunol.* 10: 460.] *Nat. Rev. Immunol.* 8: 958–969.
8. Akagawa, K. S. 2002. Functional heterogeneity of colony-stimulating factor-induced human monocyte-derived macrophages. *Int. J. Hematol.* 76: 27–34.
9. Hamilton, J. A. 2008. Colony-stimulating factors in inflammation and autoimmunity. *Nat. Rev. Immunol.* 8: 533–544.
10. Fleetwood, A. J., T. Lawrence, J. A. Hamilton, and A. D. Cook. 2007. Granulocyte-macrophage colony-stimulating factor (CSF) and macrophage CSF-dependent macrophage phenotypes display differences in cytokine profiles and transcription factor activities: implications for CSF blockade in inflammation. *J. Immunol.* 178: 5245–5252.
11. González-Domínguez, É., Á. Domínguez-Soto, C. Nieto, J. L. Flores-Sevilla, M. Pacheco-Blanco, V. Campos-Peña, M. A. Meraz-Ríos, M. A. Vega, A. L. Corbí, and C. Sánchez-Torres. 2016. Atypical activin A and IL-10 production impairs human CD16+ monocyte differentiation into anti-inflammatory macrophages. *J. Immunol.* 196: 1327–1337.
12. Sierra-Filardi, E., A. Puig-Kröger, F. J. Blanco, C. Nieto, R. Bragado, M. I. Palomero, C. Bernabéu, M. A. Vega, and A. L. Corbí. 2011. Activin A skews macrophage polarization by promoting a proinflammatory phenotype and inhibiting the acquisition of anti-inflammatory macrophage markers. *Blood* 117: 5092–5101.
13. Verreck, F. A., T. de Boer, D. M. Langenberg, M. A. Hoeve, M. Kramer, E. Vaisberg, R. Kastelein, A. Kolk, R. de Waal-Malefyt, and T. H. Ottenhoff. 2004. Human IL-23-producing type 1 macrophages promote but IL-10-producing type 2 macrophages subvert immunity to (myco)bacteria. *Proc. Natl. Acad. Sci. USA* 101: 4560–4565.
14. Cuevas, V. D., L. Anta, R. Samaniego, E. Orta-Zavalza, J. Vladimir de la Rosa, G. Baujat, Á. Domínguez-Soto, P. Sánchez-Mateos, M. M. Escribese, A. Castrillo, et al. 2017. MAFB determines human macrophage anti-inflammatory polarization: relevance for the pathogenic mechanisms operating in multicentric carpotarsal osteolysis. *J. Immunol.* 198: 2070–2081.
15. Allavena, P., A. Sica, C. Garlanda, and A. Mantovani. 2008. The Yin-Yang of tumor-associated macrophages in neoplastic progression and immune surveillance. *Immunol. Rev.* 222: 155–161.
16. Murray, P. J., J. E. Allen, S. K. Biswas, E. A. Fisher, D. W. Gilroy, S. Goerdt, S. Gordon, J. A. Hamilton, L. B. Ivashkiv, T. Lawrence, et al. 2014. Macrophage activation and polarization: nomenclature and experimental guidelines. *Immunity* 41: 14–20.
17. Soler Palacios, B., L. Estrada-Capetillo, E. Izquierdo, G. Criado, C. Nieto, C. Municio, I. González-Alvaro, P. Sánchez-Mateos, J. L. Pablos, A. L. Corbí, and A. Puig-Kröger. 2015. Macrophages from the synovium of active rheumatoid arthritis exhibit an activin A-dependent pro-inflammatory profile. *J. Pathol.* 235: 515–526.
18. Ginhoux, F., and S. Jung. 2014. Monocytes and macrophages: developmental pathways and tissue homeostasis. *Nat. Rev. Immunol.* 14: 392–404.
19. Jantsch, J., K. J. Binger, D. N. Müller, and J. Titze. 2014. Macrophages in homeostatic immune function. *Front. Physiol.* 5: 146.
20. Wynn, T. A., A. Chawla, and J. W. Pollard. 2013. Macrophage biology in development, homeostasis and disease. *Nature* 496: 445–455.
21. Bosco, M. C., M. Puppo, F. Blengio, T. Fraone, P. Cappello, M. Giovarelli, and L. Varesio. 2008. Monocytes and dendritic cells in a hypoxic environment: spotlights on chemotaxis and migration. *Immunobiology* 213: 733–749.
22. Lynn, W. A., and J. Cohen. 1995. Management of septic shock. *J. Infect.* 30: 207–212.
23. Lumeng, C. N., J. L. Bodzin, and A. R. Saltiel. 2007. Obesity induces a phenotypic switch in adipose tissue macrophage polarization. *J. Clin. Invest.* 117: 175–184.
24. Gordon, S., and F. O. Martinez. 2010. Alternative activation of macrophages: mechanism and functions. *Immunity* 32: 593–604.
25. Ruffell, B., N. I. Affara, and L. M. Coussens. 2012. Differential macrophage programming in the tumor microenvironment. *Trends Immunol.* 33: 119–126.
26. Leuschner, F., P. Dutta, R. Gorbatov, T. I. Novobrantseva, J. S. Donahoe, G. Courties, K. M. Lee, J. I. Kim, J. F. Markmann, B. Marinelli, et al. 2011. Therapeutic siRNA silencing in inflammatory monocytes in mice. *Nat. Biotechnol.* 29: 1005–1010.
27. Shechter, R., O. Miller, G. Yovel, N. Rosenzweig, A. London, J. Ruckh, K. W. Kim, E. Klein, V. Kalchenko, P. Bendel, et al. 2013. Recruitment of beneficial M2 macrophages to injured spinal cord is orchestrated by remote brain choroid plexus. *Immunity* 38: 555–569.
28. Shechter, R., and M. Schwartz. 2013. Harnessing monocyte-derived macrophages to control central nervous system pathologies: no longer 'if' but 'how'. *J. Pathol.* 229: 332–346.
29. Dou, H., C. J. Destache, J. R. Morehead, R. L. Mosley, M. D. Boska, J. Kingsley, S. Gorantla, L. Poluektova, J. A. Nelson, M. Chaubal, et al. 2006. Development of a macrophage-based nanoparticle platform for antiretroviral drug delivery. *Blood* 108: 2827–2835.
30. Almouazen, E., S. Bourgeois, A. Boussaïd, P. Valot, C. Malleval, H. Fessi, S. Nataf, and S. Briançon. 2012. Development of a nanoparticle-based system for the delivery of retinoic acid into macrophages. *Int. J. Pharm.* 430: 207–215.
31. Kazatchkine, M. D., and S. V. Kaveri. 2001. Immunomodulation of autoimmune and inflammatory diseases with intravenous immune globulin. *N. Engl. J. Med.* 345: 747–755.
32. Gelfand, E. W. 2012. Intravenous immune globulin in autoimmune and inflammatory diseases. *N. Engl. J. Med.* 367: 2015–2025.
33. Dwyer, J. M. 1996. Immunoglobulins in autoimmunity: history and mechanisms of action. *Clin. Exp. Rheumatol.* 14(Suppl. 15): S3–S7.
34. Clynes, R. 2007. IVIG therapy: interfering with interferon-gamma. *Immunity* 26: 4–6.
35. Durandy, A., S. V. Kaveri, T. W. Kuijpers, M. Basta, S. Miescher, J. V. Ravetch, and R. Rieben. 2009. Intravenous immunoglobulins–understanding properties and mechanisms. *Clin. Exp. Immunol.* 158(Suppl. 1): 2–13.
36. Schwab, I., and F. Nimmerjahn. 2013. Intravenous immunoglobulin therapy: how does IgG modulate the immune system? *Nat. Rev. Immunol.* 13: 176–189.
37. Tha-In, T., J. Bayry, H. J. Metselaar, S. V. Kaveri, and J. Kwekkeboom. 2008. Modulation of the cellular immune system by intravenous immunoglobulin. *Trends Immunol.* 29: 608–615.
38. Ballow, M. 2011. The IgG molecule as a biological immune response modifier: mechanisms of action of intravenous immune serum globulin in autoimmune and inflammatory disorders. *J. Allergy Clin. Immunol.* 127: 315–323; quiz 324–325. 10.1016/j.jaci.2010.10.030
39. Negi, V. S., S. Elluru, S. Sibéril, S. Graff-Dubois, L. Mouthon, M. D. Kazatchkine, S. Lacroix-Desmazes, J. Bayry, and S. V. Kaveri. 2007. Intravenous immunoglobulin: an update on the clinical use and mechanisms of action. *J. Clin. Immunol.* 27: 233–245.
40. Tjon, A. S., R. van Gent, T. B. Geijtenbeek, and J. Kwekkeboom. 2015. Differences in anti-inflammatory actions of intravenous immunoglobulin between mice and men: more than meets the eye. *Front. Immunol.* 6: 197.
41. Corbí, A. L., S. Sánchez-Ramón, and A. Domínguez-Soto. 2016. The potential of intravenous immunoglobulins for cancer therapy: a road that is worth taking? *Immunotherapy* 8: 601–612.
42. Ben Mkaddem, S., M. Aloulou, M. Benhamou, and R. C. Monteiro. 2014. Role of FcγRIIIA (CD16) in IVIg-mediated anti-inflammatory function. *J. Clin. Immunol.* 34(Suppl. 1): S46–S50.
43. Aloulou, M., S. Ben Mkaddem, M. Biarnes-Pelicot, T. Boussetta, H. Souchet, E. Rossato, M. Benhamou, B. Crestani, Z. Zhu, U. Blank, et al. 2012. IgG1 and IVIg induce inhibitory ITAM signaling through FcγRIII controlling inflammatory responses. *Blood* 119: 3084–3096.
44. Domínguez-Soto, A., M. de las Casas-Engel, R. Bragado, J. Medina-Echeverz, L. Aragoneses-Fenoll, E. Martín-Gayo, N. van Rooijen, P. Berraondo, M. L. Toribio, M. A. Moro, et al. 2014. Intravenous immunoglobulin promotes antitumor responses by modulating macrophage polarization. *J. Immunol.* 193: 5181–5189.
45. Dominguez-Soto, A., L. Aragoneses-Fenoll, F. Gomez-Aguado, M. T. Corcuera, J. Claria, C. Garcia-Monzon, M. Bustos, and A. L. Corbi. 2009. The pathogen receptor liver and lymph node sinusoidal endotelial cell C-type lectin is expressed in human Kupffer cells and regulated by PU.1. *Hepatology* 49: 287–296.
46. Domínguez-Soto, A., A. Puig-Kröger, M. A. Vega, and A. L. Corbí. 2005. PU.1 regulates the tissue-specific expression of dendritic cell-specific intercellular adhesion molecule (ICAM)-3-grabbing nonintegrin. *J. Biol. Chem.* 280: 33123–33131.
47. Auffray, C., M. H. Sieweke, and F. Geissmann. 2009. Blood monocytes: development, heterogeneity, and relationship with dendritic cells. *Annu. Rev. Immunol.* 27: 669–692.
48. Kaveri, S. V., M. S. Maddur, P. Hegde, S. Lacroix-Desmazes, and J. Bayry. 2011. Intravenous immunoglobulins in immunodeficiencies: more than mere replacement therapy. *Clin. Exp. Immunol.* 164(Suppl. 2): 2–5.
49. Koleba, T., and M. H. Ensom. 2006. Pharmacokinetics of intravenous immunoglobulin: a systematic review. *Pharmacotherapy* 26: 813–827.
50. Sigman, K., F. Ghibu, W. Sommerville, B. J. Toledano, Y. Bastein, L. Cameron, Q. A. Hamid, and B. Mazer. 1998. Intravenous immunoglobulin inhibits IgE production in human B lymphocytes. *J. Allergy Clin. Immunol.* 102: 421–427.

51. Lacey, D. C., A. Achuthan, A. J. Fleetwood, H. Dinh, J. Roiniotis, G. M. Scholz, M. W. Chang, S. K. Beckman, A. D. Cook, and J. A. Hamilton. 2012. Defining GM-CSF- and macrophage-CSF-dependent macrophage responses by in vitro models. *J. Immunol.* 188: 5752–5765.
52. Han, M. S., D. Y. Jung, C. Morel, S. A. Lakhani, J. K. Kim, R. A. Flavell, and R. J. Davis. 2013. JNK expression by macrophages promotes obesity-induced insulin resistance and inflammation. *Science* 339: 218–222.
53. Tanahashi, H., K. Kito, T. Ito, and K. Yoshioka. 2010. MafB protein stability is regulated by the JNK and ubiquitin-proteasome pathways. *Arch. Biochem. Biophys.* 494: 94–100.
54. Wicks, I. P., and A. W. Roberts. 2016. Targeting GM-CSF in inflammatory diseases. *Nat. Rev. Rheumatol.* 12: 37–48.
55. Biswas, S. K., and E. Lopez-Collazo. 2009. Endotoxin tolerance: new mechanisms, molecules and clinical significance. *Trends Immunol.* 30: 475–487.
56. Beutler, B. 2004. SHIP, TGF-beta, and endotoxin tolerance. *Immunity* 21: 134–135.
57. Sly, L. M., M. J. Rauh, J. Kalesnikoff, C. H. Song, and G. Krystal. 2004. LPS-induced upregulation of SHIP is essential for endotoxin tolerance. *Immunity* 21: 227–239.
58. Boone, D. L., E. E. Turer, E. G. Lee, R. C. Ahmad, M. T. Wheeler, C. Tsui, P. Hurley, M. Chien, S. Chai, O. Hitotsumatsu, et al. 2004. The ubiquitin-modifying enzyme A20 is required for termination of Toll-like receptor responses. [Published erratum appears in 2005 *Nat. Immunol.* 6: 114.] *Nat. Immunol.* 5: 1052–1060.
59. An, H., J. Hou, J. Zhou, W. Zhao, H. Xu, Y. Zheng, Y. Yu, S. Liu, and X. Cao. 2008. Phosphatase SHP-1 promotes TLR- and RIG-I-activated production of type I interferon by inhibiting the kinase IRAK1. *Nat. Immunol.* 9: 542–550.
60. Anthony, R. M., T. Kobayashi, F. Wermeling, and J. V. Ravetch. 2011. Intravenous gammaglobulin suppresses inflammation through a novel T(H)2 pathway. *Nature* 475: 110–113.
61. Campbell, I. K., S. Miescher, D. R. Branch, P. J. Mott, A. H. Lazarus, D. Han, E. Maraskovsky, A. W. Zuercher, A. Neschadim, D. Leontyev, et al. 2014. Therapeutic effect of IVIG on inflammatory arthritis in mice is dependent on the Fc portion and independent of sialylation or basophils. *J. Immunol.* 192: 5031–5038.
62. Fleetwood, A. J., H. Dinh, A. D. Cook, P. J. Hertzog, and J. A. Hamilton. 2009. GM-CSF- and M-CSF-dependent macrophage phenotypes display differential dependence on type I interferon signaling. *J. Leukoc. Biol.* 86: 411–421.
63. Nimmerjahn, F., and J. V. Ravetch. 2008. Anti-inflammatory actions of intravenous immunoglobulin. *Annu. Rev. Immunol.* 26: 513–533.
64. Nimmerjahn, F., and J. V. Ravetch. 2007. Fc-receptors as regulators of immunity. *Adv. Immunol.* 96: 179–204.
65. Fishman, P., S. Bar-Yehuda, and Y. Shoenfeld. 2002. IVIg to prevent tumor metastases (Review). *Int. J. Oncol.* 21: 875–880.
66. Sapir, T., and Y. Shoenfeld. 2005. Uncovering the hidden potential of intravenous immunoglobulin as an anticancer therapy. *Clin. Rev. Allergy Immunol.* 29: 307–310.
67. Lee, M. J., E. Lim, S. Mun, S. Bae, K. Murata, L. B. Ivashkiv, and K. H. Park-Min. 2016. Intravenous immunoglobulin (IVIG) attenuates TNF-induced pathologic bone resorption and suppresses osteoclastogenesis by inducing A20 expression. *J. Cell. Physiol.* 231: 449–458.
68. Xia, Y., and A. L. Schneyer. 2009. The biology of activin: recent advances in structure, regulation and function. *J. Endocrinol.* 202: 1–12.
69. Sozzani, S., and T. Musso. 2011. The yin and yang of activin A. *Blood* 117: 5013–5015.
70. Florio, P., M. Gabbanini, L. E. Borges, L. Bonaccorsi, S. Pinzauti, F. M. Reis, P. Boy Torres, G. Rago, P. Litta, and F. Petraglia. 2010. Activins and related proteins in the establishment of pregnancy. *Reprod. Sci.* 17: 320–330.
71. Manfredi, G., L. Dell'Aera, and R. Liguori. 2015. Overcoming recurrent spontaneous abortions in women suffering from IgG subclass deficiency: high efficiency of low dose intravenous immunoglobulins treatment. *Eur. Ann. Allergy Clin. Immunol.* 47: 91–94.
72. Ramos-Medina, R., A. García-Segovia, J. Gil, J. Carbone, A. Aguarón de la Cruz, A. Seyfferth, B. Alonso, J. Alonso, J. A. León, D. Alecsandru, et al. 2014. Experience in IVIg therapy for selected women with recurrent reproductive failure and NK cell expansion. *Am. J. Reprod. Immunol.* 71: 458–466.
73. Loubaki, L., D. Chabot, and R. Bazin. 2015. Involvement of the TNF-α/TGF-β/IDO axis in IVIg-induced immune tolerance. *Cytokine* 71: 181–187.
74. Ibanez, C., P. Sune, A. Fierro, S. Rodriguez, M. Lopez, A. Alvarez, J. De Gracia, and J. B. Montoro. 2005. Modulating effects of intravenous immunoglobulins on serum cytokine levels in patients with primary hypogammaglobulinemia. *BioDrugs* 19: 59–65.
75. Leung, D. Y. 1989. The immunologic effects of IVIG in Kawasaki disease. *Int. Rev. Immunol.* 5: 197–202.
76. Dace, D. S., A. A. Khan, J. L. Stark, J. Kelly, A. H. Cross, and R. S. Apte. 2009. Interleukin-10 overexpression promotes Fas-ligand-dependent chronic macrophage-mediated demyelinating polyneuropathy. *PLoS One* 4: e7121.

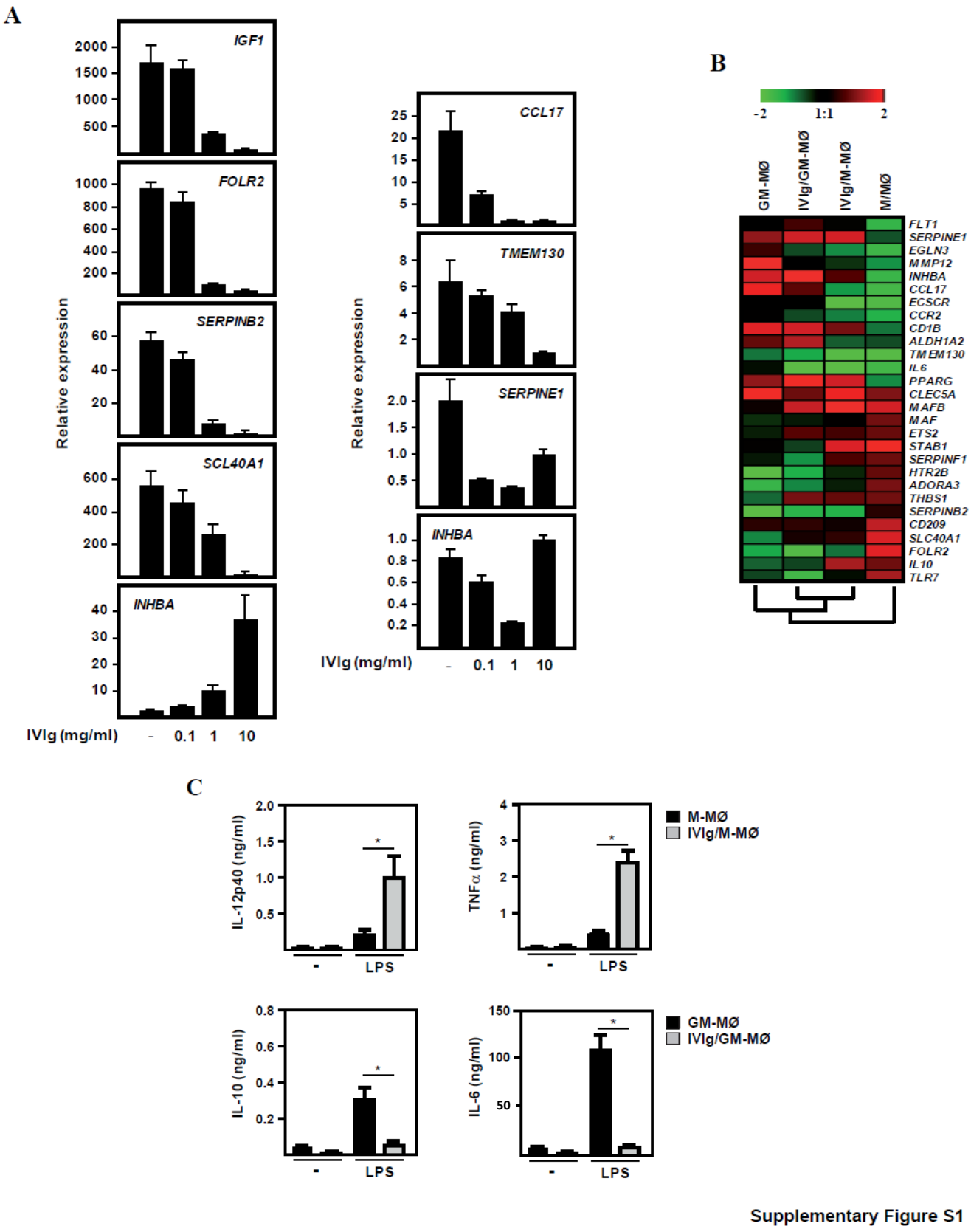

Supplementary Figure S1

Supplementary Figure S1. (A) Dose-response effect of IVIg on the acquisition of human macrophage polarization-specific genes. Expression of the indicated genes in M-MØ (left panels) and GM-MØ (right panels) generated in the absence (-) or in the continuous presence of increasing IVIg concentrations, as determined by qRT-PCR. Results are expressed as Relative Expression (relative to GAPDH mRNA levels). Each determination was done in triplicate on two independent monocyte samples, and the mean ± SD from one of the experiments is shown. **(B)** Non-supervised hierarchical clustering (Genesis software, http://genome.tugraz.at/genesisclient/genesisclient_description.shtml) on the mean expression level of the indicated genes in M-MØ, IVIg/M-MØ, GM-MØ and IVIg/GM-MØ from five independent donors. **(C)** Production of IL-12p40 and TNFα in M-MØ and IVIg/M-MØ (upper panels), and IL-10 and IL-6 in GM-MØ and IVIg/GM-MØ (lower panels) that were either left untreated (-) or stimulated with 10 ng/ml LPS for 24 hours, as determined by ELISA. Each determination was done in triplicate, and shown are the mean ± SEM of three independent experiments (*, $p<0.05$).

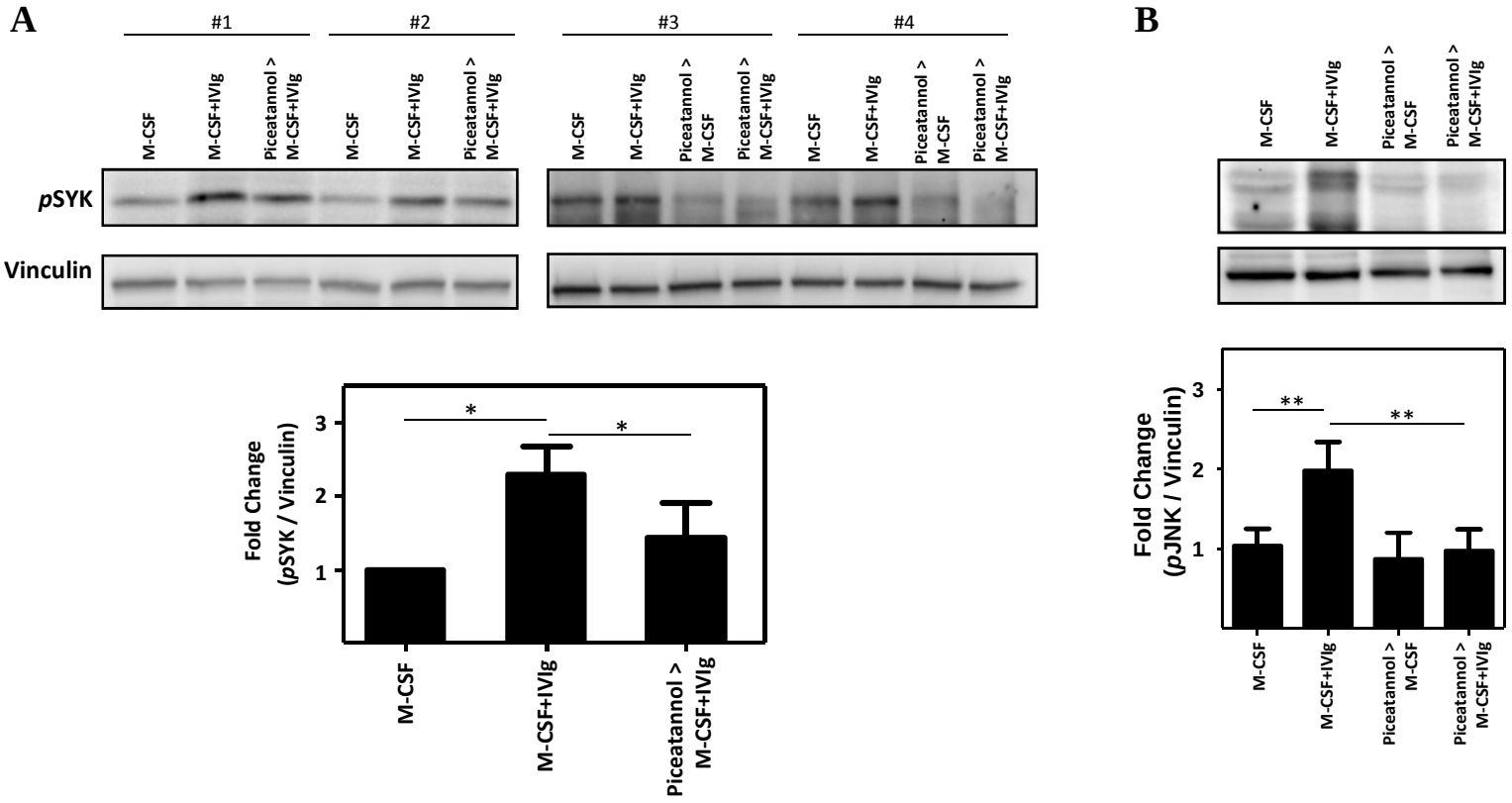

Supplementary Figure S2

Supplementary Figure S2. **(A)** (Upper panel) Immunoblot analysis of *p*SYK protein levels in monocytes subjected to the indicated treatments. Cells were treated or not with 80 μM piceatannol 1 hour before M-CSF or M-CSF+IVIg treatment. After 10 minutes, cells were lysed and protein levels *p*SYK and vinculin were determined. Four independent experiments were performed and all of them are shown. (Lower panel) Determination of the relative *p*Syk protein levels in the four independent experiments shown in the Upper panel as determined by densitometric quantification (*, $p<0.05$). **(B)** (Upper panel) Immunoblot analysis of *p*JNK protein levels in monocytes subjected to the indicated treatments. Cells were treated or not with 80 μM piceatannol 1 hour before M-CSF or M-CSF+IVIg treatment. After 20 minutes, cells were lysed and protein levels *p*JNK and vinculin were determined. Three independent experiments were performed and one of them is shown. (Lower panel) Determination of the relative *p*JNK protein levels in three independent experiments identical to the one shown in the Upper panel, as determined by densitometric quantification (**, $p<0.01$).